REPORT

EXOPLANETS

Oxygen fugacities of extrasolar rocks: Evidence for an Earth-like geochemistry of exoplanets

Alexandra E. Doyle[1]*, Edward D. Young[1]*, Beth Klein[2], Ben Zuckerman[2], Hilke E. Schlichting[1,2,3]

Oxygen fugacity is a measure of rock oxidation that influences planetary structure and evolution. Most rocky bodies in the Solar System formed at oxygen fugacities approximately five orders of magnitude higher than a hydrogen-rich gas of solar composition. It is unclear whether this oxidation of rocks in the Solar System is typical among other planetary systems. We exploit the elemental abundances observed in six white dwarfs polluted by the accretion of rocky bodies to determine the fraction of oxidized iron in those extrasolar rocky bodies and therefore their oxygen fugacities. The results are consistent with the oxygen fugacities of Earth, Mars, and typical asteroids in the Solar System, suggesting that at least some rocky exoplanets are geophysically and geochemically similar to Earth.

Estimating the composition of extrasolar planets from host-star abundances or from planet mass-radius relationships is difficult and unreliable (*1*, *2*). The elemental abundances in some white dwarfs (WDs) provide an alternative, more direct approach for determining the composition of extrasolar rocks. WDs are the remnant cores left behind when a star ejects its hydrogen-rich outer layers after the red giant phase. These remnant cores are ~0.5 $M_\odot$ (solar masses) and about the same radius as Earth, are no longer powered by fusion, and slowly cool over time. Because of their high densities, and thus strong gravitational fields, elements heavier than helium rapidly sink below their surfaces, becoming unobservable. Nonetheless, spectroscopic studies show that the atmospheres of up to half of WDs with effective temperatures <25,000 K are "polluted" by elements heavier than He (*3*–*5*). The source of these heavy elements is exogenous, coming from accretion of debris from rocky bodies that previously orbited the WDs (*6*–*9*). We exploit this pollution to measure the elemental constituents of extrasolar rocky bodies. We collated observations from the literature of polluting elements in six WDs: SDSS J104341.53+085558.2 (*10*), SDSS J122859.92+104033.0 (*9*), SBSS 1536+520 (*11*), GD 40 (*8*, *12*), SDSS J073842.56+183509.6 (*13*), and LBQS 1145+0145 (*14*) (hereafter, SDSS J1043+0855, WD 1226+110, WD 1536+520, GD 40, SDSS J0738+1835, and WD 1145+017, respectively). Their coordinates are listed in table S1. The bulk compositions of the bodies polluting these WDs resemble those of rocky bodies in the Solar System (*15*, *16*) (Fig. 1).

We use the relative abundances of rock-forming elements in polluted WDs to determine the effective partial pressure of oxygen, i.e., the oxygen fugacity (f_{O_2}) of the accreted rocks. Oxygen fugacity is a measure of the degree of oxidation in the rocks. It corresponds to the effective partial pressure of gaseous oxygen that would be in thermodynamic equilibrium with the material of interest. In combination with other factors, the intrinsic oxygen fugacity of a planet will determine the relative size of its metallic core, the geochemistry of its mantle and crust, the composition of its atmosphere, and the forces responsible for mountain building (*17*, *18*). Oxygen fugacity is also thought to be among the parameters that determine the habitability of a planet (*19*). In practice, f_{O_2} is usually expressed as the nonideal partial pressure of oxygen relative to a convenient reference value.

Oxygen fugacities of rocky planets are often reported relative to the reference Iron-Wüstite (IW) equilibrium reaction Fe (Iron) + ½ O_2 = FeO (Wüstite), such that $\Delta IW \equiv \log(f_{O_2}) - \log(f_{O_2})_{IW}$ (*16*). When expressed this way, differences in oxygen fugacity are nearly independent of temperature and pressure (*16*). The initial oxidation state of a rocky body with at least some Fe metal at the time of its formation is recorded by the concentration of oxidized iron (hereafter denoted as FeO, although it may include other oxides of iron) in the rock and the concentration of Fe in the metal

$$\Delta IW = 2\log\left(\frac{x_{FeO}^{rock}}{x_{Fe}^{metal}}\right) + 2\log\left(\frac{\gamma_{FeO}^{rock}}{\gamma_{Fe}^{metal}}\right) \quad (1)$$

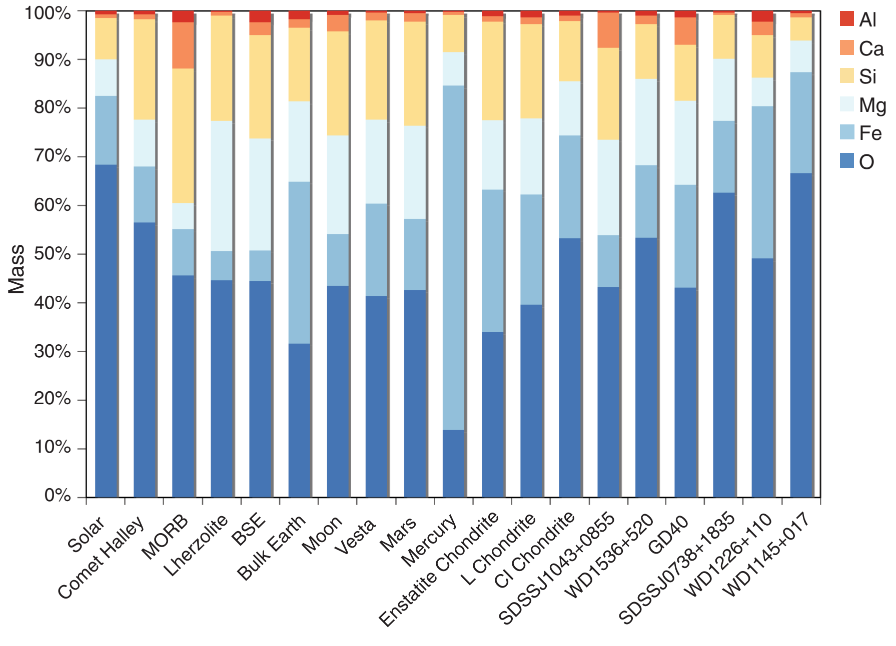

Fig. 1. Bulk compositions by mass for six white dwarfs compared with Solar System bodies. Bulk compositions of the six rock-forming elements Al, Ca, Si, Mg, Fe, and O are indicated by the colored bars. The six white dwarfs are shown in the right-most columns. Shown for comparison are Solar System objects: the Sun, Comet Halley (1P/Halley), Earth, the Moon, Vesta, Mars, Mercury, three types of meteorites (enstatite chondrite, ordinary L chondrite, and carbonaceous CI chondrite), and three terrestrial igneous rock types [mid ocean ridge basalt (MORB), lherzolite (representing Earth's mantle), and bulk silicate Earth (BSE)] (*16*). The relatively high abundances of Fe in bulk Mercury and bulk Earth are due to their metal cores. The compositions of the white dwarfs are similar to the Solar System rocks. The large amount of O in WD 1145+017 is highly uncertain. Values are listed in data S1.

[1]Department of Earth, Planetary, and Space Sciences, University of California, Los Angeles, Los Angeles, CA, USA. [2]Department of Physics and Astronomy, University of California, Los Angeles, Los Angeles, CA, USA. [3]Department of Earth, Atmospheric and Planetary Sciences, Massachusetts Institute of Technology, Cambridge, MA, USA.
***Corresponding author. Email: a.doyle@ucla.edu (A.E.D.); eyoung@epss.ucla.edu (E.D.Y.)**

where x_i^k are mole fractions of the species i in phase k, γ_i^k are activity coefficients for the species, and thermodynamic activities are $a_i^k = x_i^k \gamma_i^k$. To facilitate comparison, we set the uncertain activity coefficients to unity, so the second term on the right-hand side of Eq. 1 vanishes. Equation 1 expresses the f_{O_2} at the time the planet or planetesimal formed (*20*, *21*); we refer to this as the intrinsic oxygen fugacity of the body. The partitioning of iron between rock and metal during formation leaves a record of the intrinsic oxygen fugacity in the form of the mole fraction of FeO in the rocks, x_{FeO}^{rock}. This signature persists even after the rock and metal are separated by the process of differentiation (partitioning between core and mantle). This is because changes in the valence state of iron during subsequent reactions proceed without appreciably altering the total amount of iron bonded to oxygen in the rocks. For example, the reaction

$$2Fe^{2+}Fe_2^{3+}O_4{}^{spinel} + 6Fe^{2+}SiO_3{}^{pyroxene} \rightleftharpoons 6Fe_2^{2+}O_4{}^{olivine} + O_2 \quad (2)$$

determines the Fe^{3+}/Fe^{2+} ratio, and thus the f_{O_2}, in a rock containing the minerals spinel, pyroxene, and olivine, without substantially altering the total Fe bonded to oxygen (from 2.17 oxygens per Fe to 2.00 oxygens per Fe). Reactions like these that follow the formation of a rocky body lead to local variations in f_{O_2} within the body but do not generally alter the intrinsic oxygen fugacity recorded by application of Eq. 1 (Fig. 2). The intrinsic oxygen fugacity of Earth is constrained by $x_{FeO}^{mantle} = 0.06$ [8 wt % (weight percent) FeO] in its mantle and the composition of its Fe-rich core. This leads to a terrestrial ΔIW value of about –1 to –2, with the range due to the uncertain values for the activity coefficient ratio [commonly used values of $\gamma_{FeO}{}^{mantle}/\gamma_{Fe}{}^{core}$ range from ~1 to 4 (*22*)].

The material accreted by the six polluted WDs in this study are rocks devoid of metal, as demonstrated by the lack of excess Fe relative to oxygen (Fig. 1). Separation of metal and rock during accretion onto WDs is suggested by the ranges in element ratios in polluted WDs (*23*) and from observations of a metal-density planetesimal core orbiting a WD (*24*). Our f_{O_2} measurements are representative of the fugacity values at the time of core formation, even though they are derived from crustal or mantle rocks. The maximum intrinsic oxygen fugacity calculated from Eq. 1 approaches 0 as the mole fraction of Fe in the silicate increases. Values for ΔIW greater than ~–0.9 for elemental concentrations similar to Solar System rocks imply that all of the iron has been oxidized, and that the intrinsic ΔIW values from Eq. 1 are therefore minimum estimates for the oxidation state at the time the rocks formed.

The solar protoplanetary disk must, on average, have had the same composition as the Sun (see supplementary text in the supplementary materials). The oxygen fugacity of a gas with solar composition is determined by its H_2O/H_2 ratio, after correcting for the oxygen bound to carbon in CO and other less abundant oxides, according to the reaction $H_2 + ½ O_2 \rightleftharpoons H_2O$ (*16*). Studies of meteorites reveal that, like Earth, most rocky bodies in the Solar System formed with ΔIW approximately five orders of magnitude higher than that of a solar gas (*25*, *26*) (Fig. 3). The presence of large amounts of iron bonded to oxygen in silicates in chondrite meteorites indicates there was a relatively high oxygen fugacity during the earliest stages of rock formation in the Solar System (*27*). The enhancement in oxygen fugacity during rocky body formation may be attributable to the sublimation of water-rich and/or rock-rich dust at high dust/gas ratios (*28*). In this context, we examine whether the processes that led to oxidation of rocks in the Solar System are typical of other planetary systems, and therefore whether the geophysical and geochemical characteristics of Earth are likely to be common among rocky exoplanets.

When the six major rock-forming elements are measured in a polluted WD, the abundance of FeO may be used to determine the oxidation state of the accreted exoplanetary rocky bodies (*2*, *8*, *29*). Polluted WDs with observed abundances of O, Mg, Si, Fe, Al, and Ca can be used to calculate oxygen fugacities from Eq. 1 by recognizing that any Fe not bonded to oxygen must have existed as metal in the accreted bodies. Data for polluted WDs are preferable to elemental abundances in other stars because of the known rocky provenance of the accreted elements in WDs, especially in the case of oxygen.

Our basic methodology is as follows: The oxide components MgO, SiO_2, FeO, Al_2O_3, and CaO describe the compositions of the major minerals that make up the accreting rocks. By assigning oxygen first to Mg, then Si, Al, Ca, and finally Fe, we calculate the relative amount of oxidized Fe, as FeO, and assign any remaining Fe to metal representing the core of the body (*2*, *8*, *30*). We propagate measurement uncertainties for the polluted WDs using a Monte Carlo bootstrap approach (*16*).

We validated our method using Solar System bodies by converting the composition of these bodies into hypothetical polluted WDs, as if rocks from the bodies (e.g., Earth, Mars, Mercury) had accreted onto a WD. We used typical WD measurement uncertainties for these calculations and recovered the known intrinsic

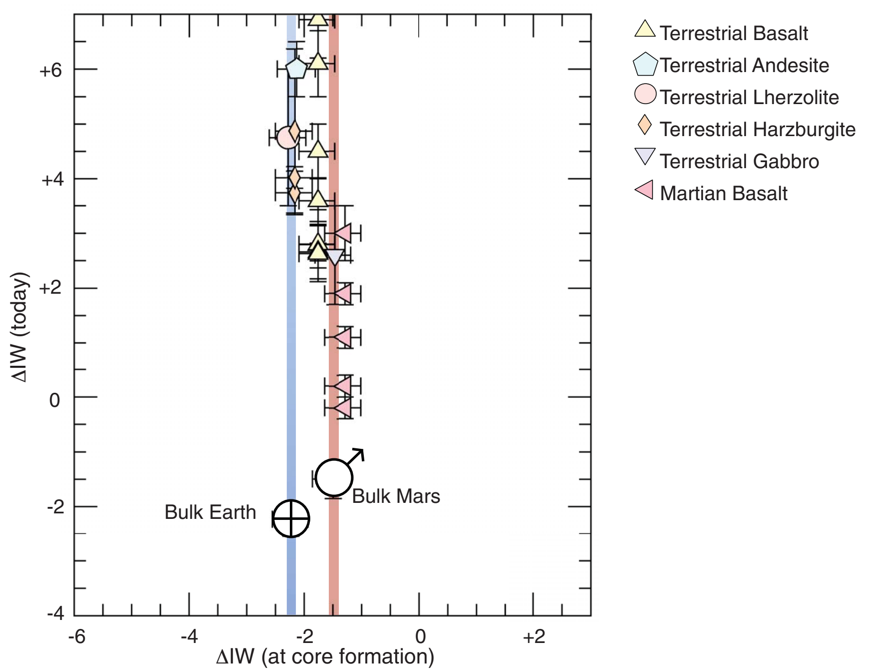

Fig. 2. Oxygen fugacities relative to IW at core formation versus today. Terrestrial and Martian rocks are characterized by ΔIW at the time of core formation, as calculated from the concentration of FeO, and ΔIW as measured today using various other measures of oxygen fugacity (*16*). Bulk Earth and bulk Mars values are also shown, demonstrating their similarity in intrinsic ΔIW at the time of core formation, despite the ranges in ΔIW as measured today. Error bars are 1σ (*16*). Where oxygen fugacities were previously reported relative to the quartz-fayalite-magnetite buffer (QFM), we converted them using ΔIW = ΔQFM – 4. Andesite, basalt, and gabbro represent crustal rocks, whereas lherzolite and harzburgite, specific types of peridotites, are mantle rocks.

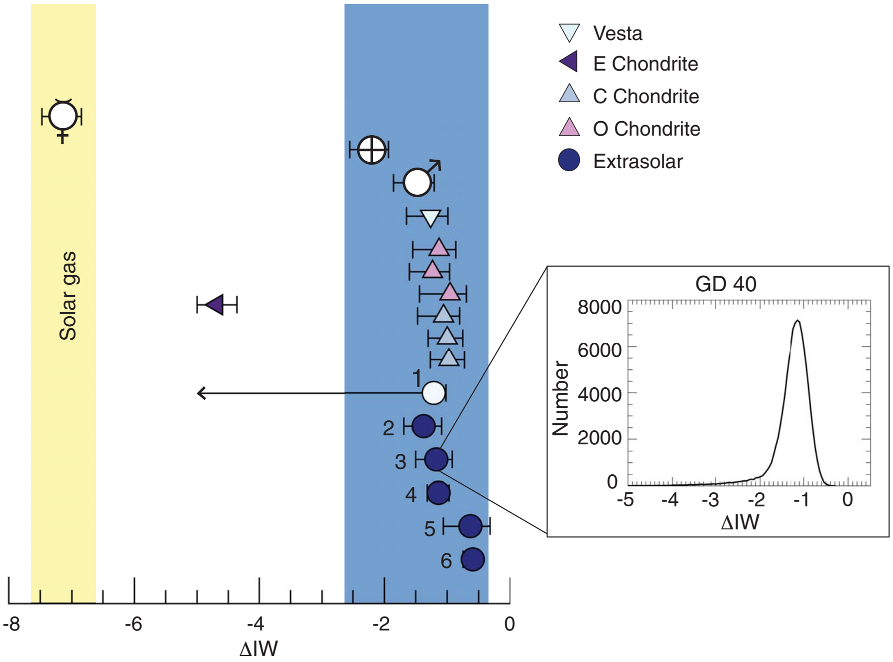

Fig. 3. Calculated oxygen fugacities relative to IW for rocky extrasolar bodies. Numbered circles show the values for rocky debris that polluted the white dwarfs: (1) SDSS J1043+0855; (2) WD 1536+520; (3) GD 40; (4) SDSS J0738+1835; (5) WD 1226+110; and (6) WD 1145+017. Values are listed in table S1. Error bars (1σ) are from propagation of measurement uncertainties (*16*). Only an upper limit could be obtained for SDSS J1043+0855 owing to the measurement uncertainties relative to the Fe concentration for that star (*16*). The ranges of relative oxygen fugacities for a gas of solar composition (yellow) and for most Solar System rocky bodies (blue) are shown for comparison. Rocks from Solar System planets are also shown and are represented by their planet symbols: Earth (⊕), Mars (♂), and Mercury (☿). Triangles show values for meteorites, representing bodies in the asteroid belt, including Vesta. The inset shows an example ΔIW probability distribution for one of the WDs, GD 40 (*16*); equivalents for the other WDs are shown in fig. S3.

oxygen fugacities for Earth, Mars, Mercury, Vesta, and various chondritic bodies (*16*). The Solar System bodies span a range in ΔIW of ~6 dex, in agreement with previous studies showing that Mercury and enstatite meteorites have f_{O_2} orders of magnitude lower than those for Earth, Mars, and other chondrite group meteorites (*31*, *32*).

The six WDs in this study were chosen because quantitative measurements of all six major rock-forming elements are available for each. These WDs also exhibit infrared excesses, indicative of surrounding debris disks (*6*). The ΔIW values we obtain for the rocks accreted by the polluted WDs are all similar to those of Earth, Mars, Vesta, and the asteroids represented by carbonaceous (C) and ordinary (O) chondrites in the Solar System (Fig. 3).

In cases where there is both more oxygen than required to oxidize all other major elements and a commensurate amount of hydrogen, water in the accreting body is implied and the partitioning of oxygen between ice and Fe can be ambiguous (*33*, *34*). In addition, unaccounted-for Si in metal cores may have liberated oxygen to oxidize Fe in the accreted bodies. We find that these effects are small for the WDs in this study and do not affect the elemental abundances we used to derive oxygen fugacities (*16*) (fig. S5).

The high oxygen fugacities of these extrasolar rocks, relative to a solar gas, suggest that whatever process oxidized rock-forming materials in the Solar System also operated in these other planetary systems. The large amount of oxidized iron in chondrite meteorites shows that oxidation relative to a solar gas occurred early in the Solar System, evidently before, or during the earliest stages of, planetesimal formation. Raising ΔIW by 5 log units, from solar to rock-like values, requires the gas to acquire an H_2O/H_2 ratio ~400 times that of a solar gas (*28*). This enrichment factor is greater than can be explained by simply transporting water in the form of ice particles from the outer to the inner Solar System (*28*). If dust/gas ratios control the oxidation states during rock formation, we conclude that the Solar System and the planetary systems around these six polluted WDs had similar ratios. This implies that high dust/gas ratios are intrinsic to rock formation in protoplanetary disks. A similar compositional link between planet formation in the Solar System and that around other stars is indicated by the depletion of carbon in both solar and extrasolar rocks (*35*, *36*).

The high oxidation state of these rocks determined the mineralogy, and therefore the geophysical behavior, of their parent bodies or the planets these bodies formed. For example, the lower mantle of Earth is composed of ~70% bridgmanite and ~20% magnesiowüstite, two mineral phases with markedly different rheological properties whose abundances depend on f_{O_2}. The relative abundances of these minerals determine the dynamic behavior of the mantle (*37*). For illustration, the influence of oxygen fugacity on the mineralogy of a silicate mantle, and the composition of a metal-rich core, can be described by the reaction

$$\mathrm{MgO}^{\mathrm{magnesiowüstite}} + \mathrm{Si}^{\mathrm{core}} + \mathrm{O}_2 \rightleftharpoons \mathrm{MgSiO_3}^{\mathrm{bridgmanite}} \quad (3)$$

where MgO refers to the Mg component in mantle magnesiowüstite [(Mg,Fe)O], $MgSiO_3$ refers to the Mg component (bridgmanite) in mantle silicate perovskite [$(Mg,Fe)SiO_3$], and Si^{core} refers to Si in the metal-rich core. Rearranging the equilibrium constant for the reaction in Eq. 3, $k_{\mathrm{Eq.\ 2}}$, shows that the activity ratio of bridgmanite to magnesiowüstite is expected to vary with oxygen fugacity

$$f_{O_2} = \frac{a^{\mathrm{bridgmanite}}_{\mathrm{MgSiO_3}}}{a^{\mathrm{magnesiowüstite}}_{\mathrm{MgO}}\ a^{\mathrm{core}}_{\mathrm{Si}}\ k_{\mathrm{Eq.2}}} \quad (4)$$

Equation 4 also illustrates that the Si content of the core varies inversely with oxygen fugacity. The concentrations of Si and other light elements in the core likely play a role in driving the compositional convection within the core that powers Earth's magnetic field (*38*, *39*), which affects a planet's habitability (*40*). The relative size of the metallic core of a body (or even its existence) is also determined by oxygen fugacity (*41*). If the body or bodies that accreted onto WD 1536+520 were otherwise similar to Earth or its antecedents, the ΔIW value of –1.37 would result in a planet with an Fe-rich metal core making up ~20% of the mass of the parent body. For comparison, the most highly oxidized bodies we found, with ΔIW ~ –0.6, would assemble to form a planet with no Fe-rich metal core.

Our results show that the parent objects that polluted these WDs had intrinsic oxidation states similar to those of rocks in the Solar System. Based on estimates of their mass, the bodies accreting onto WDs were either asteroids that represent the building blocks of rocky exoplanets, or they were fragments of rocky exoplanets themselves (*15*, *42*). In either case, our results constrain the intrinsic oxygen fugacities of rocky bodies that orbited the progenitor star of their host WD. Our data indicate that rocky exoplanets constructed from these planetesimals should be geophysically and geochemically similar to rocky planets in the Solar System, including Earth.

REFERENCES AND NOTES

1. A. Gupta, H. E. Schlichting, *Mon. Not. R. Astron. Soc.* **487**, 24–33 (2019).
2. C. T. Unterborn, W. R. Panero, *Astrophys. J.* **845**, 61 (2017).
3. B. Zuckerman, D. Koester, I. N. Reid, M. Hunsch, *Astrophys. J.* **596**, 477–495 (2003).
4. B. Zuckerman, C. Melis, B. Klein, D. Koester, M. Jura, *Astrophys. J.* **722**, 725–736 (2010).
5. D. Koester, B. T. Gansicke, J. Farihi, *Astron. Astrophys.* **566**, A34 (2014).
6. M. Jura, *Astrophys. J.* **584**, L91–L94 (2003).
7. B. Zuckerman, D. Koester, C. Melis, B. M. Hansen, M. Jura, *Astrophys. J.* **671**, 872–877 (2007).
8. B. Klein, M. Jura, D. Koester, B. Zuckerman, C. Melis, *Astrophys. J.* **709**, 950–962 (2010).
9. B. T. Gänsicke, D. *et al*., *Mon. Not. R. Astron. Soc.* **424**, 333–347 (2012).
10. C. Melis, P. Dufour, *Astrophys. J.* **834**, 1 (2016).
11. J. Farihi *et al*., *Mon. Not. R. Astron. Soc.* **463**, 3186–3192 (2016).
12. M. Jura, S. Xu, B. Klein, D. Koester, B. Zuckerman, *Astrophys. J.* **750**, 69 (2012).
13. P. Dufour *et al*., *Astrophys. J.* **749**, 6 (2012).
14. S. Xu, M. Jura, P. Dufour, B. Zuckerman, *Astrophys. J.* **816**, L22 (2016).
15. M. Jura, E. D. Young, *Annu. Rev. Earth Planet. Sci.* **42**, 45–67 (2014).
16. Materials and methods are available as supplementary materials.
17. D. T. Wetzel, M. J. Rutherford, S. D. Jacobsen, E. H. Hauri, A. E. Saal, *Proc. Natl. Acad. Sci. U.S.A.* **110**, 8010–8013 (2013).
18. K. Putirka, *Am. Mineral.* **101**, 819–840 (2016).
19. B. L. Ehlmann *et al*., *J. Geophys. Res. Planets* **121**, 1927–1961 (2016).
20. J. Siebert, J. Badro, D. Antonangeli, F. J. Ryerson, *Science* **339**, 1194–1197 (2013).
21. D. C. Rubie, C. K. Gessmann, D. J. Frost, *Nature* **429**, 58–61 (2004).
22. M. K. Jordan, H. Tang, I. E. Kohl, E. D. Young, *Geochim. Cosmochim. Acta* **246**, 461–477 (2019).
23. M. Jura, E. D. Young, *Annu. Rev. Earth Planet. Sci.* **42**, 45–67 (2014).
24. C. J. Manser *et al*., *Science* **364**, 66–69 (2019).
25. J. I. Simon *et al*., *Earth Planet. Sci. Lett.* **238**, 272–283 (2005).
26. L. Grossman, J. R. Beckett, A. V. Fedkin, S. B. Simon, F. J. Ciesla, *Rev. Mineral. Geochem.* **68**, 93–140 (2008).
27. L. Grossman, A. V. Fedkin, S. B. Simon, *Meteorit. Planet. Sci.* **47**, 2160–2169 (2012).
28. J. Monteux, G. J. Golabek, D. C. Rubie, G. Tobie, E. D. Young, *Space Sci. Rev.* **214**, 39 (2018).
29. D. C. Rubie *et al*., *Earth Planet. Sci. Lett.* **301**, 31–42 (2011).
30. M. Asplund, N. Grevesse, A. J. Sauval, *Nucl. Phys. A* **777**, 1–4 (2006).
31. L. R. Nittler, S. Z. Weider, *Elements* **15**, 33–38 (2019).
32. C. Cartier, B. J. Wood, *Elements* **15**, 39–45 (2019).
33. J. Farihi, B. T. Gänsicke, D. Koester, *Science* **342**, 218–220 (2013).
34. R. Raddi *et al*., *Mon. Not. R. Astron. Soc.* **450**, 2083–2093 (2015).
35. M. Jura, *Astrophys. J.* **653**, 613–620 (2006).
36. J.-E. Lee, E. A. Bergin, H. Nomura, *Astrophys. J.* **710**, L21–L25 (2010).
37. J. Girard, G. Amulele, R. Farla, A. Mohiuddin, S. Karato, *Science* **351**, 144–147 (2016).
38. G. Helffrich, *Earth Planet. Sci. Lett.* **391**, 256–262 (2014).
39. D. Gubbins, *Q. J. R. Astron. Soc.* **32**, 69–84 (1991).
40. P. Cuartas-Restrepo, *Open Astron.* **27**, 183–231 (2018).
41. L. T. Elkins-Tanton, S. Seager, *Astrophys. J.* **688**, 628–635 (2008).
42. J. Farihi *et al*., *Mon. Not. R. Astron. Soc.* **424**, 464–471 (2012).

ACKNOWLEDGMENTS

This paper benefited from the comments provided by three anonymous reviewers. **Funding:** E.D.Y. acknowledges support from the NASA Exoplanets program grant NNX16AB53G. A.E.D. acknowledges financial support from NASA Space Grant. H.E.S. gratefully acknowledges support from the National Aeronautics and Space Administration under grant 17 NAI18_2-0029 issued through the NExSS Program. **Author contributions:** A.E.D. performed the calculations and co-wrote the manuscript. E.D.Y. conceived of the project, supervised the calculations, and co-wrote the manuscript. B.Z. and B.K. analyzed the WD data. H.E.S. contributed to the statistical analysis. All authors contributed to the interpretation of the data and the preparation of the paper. **Competing interests:** The authors declare no competing interests. **Data and materials availability:** Input compositional data are available in data S1 and our derived oxygen fugacities are listed in table S1. The bootstrap and analytical data analysis codes are available as data S2 and S3.

SUPPLEMENTARY MATERIALS

science.sciencemag.org/content/366/6463/356/suppl/DC1
Materials and Methods
Supplementary Text
Figs. S1 to S6
Table S1
References (*43*–*71*)
Data S1 to S3

19 March 2019; accepted 20 September 2019
10.1126/science.aax3901

Science

Oxygen fugacities of extrasolar rocks: Evidence for an Earth-like geochemistry of exoplanets

Alexandra E. Doyle, Edward D. Young, Beth Klein, Ben Zuckerman and Hilke E. Schlichting

Science **366** (6463), 356-359.
DOI: 10.1126/science.aax3901

Peering inside extrasolar rocky bodies

The oxygen fugacity of a rock, f_{O2}, is a measure of how oxidizing or reducing its surroundings were when the rock formed. Different minerals form at different f_{O2} and have different physical properties, so the internal structure of an exoplanet depends on this value. Doyle *et al.* exploited the signature left behind when rocky bodies impact a white dwarf—the remnant of a dead star. By examining the rock-forming elements left on the surface of each white dwarf, they determine f_{O2} in the impacting body. Six systems all had similar f_{O2} to bodies in the Solar System, consistent with the idea that rocky exoplanets often have internal properties similar to those of Earth and Mars.

Science, this issue p. 356

Science (print ISSN 0036-8075; online ISSN 1095-9203) is published by the American Association for the Advancement of Science, 1200 New York Avenue NW, Washington, DC 20005. The title *Science* is a registered trademark of AAAS.